DOI: 10.1478/AAPP.97S1A14

AAPP | Atti della Accademia Peloritana dei Pericolanti
Classe di Scienze Fisiche, Matematiche e Naturali
ISSN 1825-1242

Vol. 97, No. S1, A14 (2019)

EFFECTIVE THERMAL CONDUCTIVITY OF NANOSTRUCTURES: A REVIEW

GEORGY LEBON [a*] AND HATIM MACHRAFI [a]

ABSTRACT. We present a synthesis of recent results on thermal heat conductivity in nano-composites and nano-structures. The model is a mixt of the Effective Medium Approximation (EMA) and Extended Irreversible Thermodynamics (EXIT). The latter is particularly well adapted to the description of small scaled systems and will be used to derive the expression of the thermal conductivity of nanoparticles. The model is applied to spherical, cylindrical (nanowires) and porous nanoparticles, respectively, being embedded in host media, like polymeric matrices and semi-conductors. Good agreement is observed with other models, experimental data and Monte-Carlo simulations.

1. Introduction

It was observed experimentally that dispersion of nanoparticles, *i.e.*, small-size particles of the order of 5 nm to 100 nm, in some classes of materials (like polymers or semi-conductors), modifies considerably their mechanical and thermal properties. In the foregoing, we focus on thermal transport, ignoring mechanical properties, and limit our analysis to non-metallic bodies so that the heat carriers are exclusively phonons, in metallic materials electrons will contribute to the heat transport, while in semi-metals, both phonons and electrons participate to heat conduction. The aim of this work is to propose a general and systematic theoretical frame for predicting the thermal conductivity of nanocomposites; in particular, we will discuss the role of various specific parameters as

- The nature, shape and size of the embedded nanoparticles.
- The volume fraction of particles.
- The thermal properties of host medium and particles.
- The temperature of the system.
- The porosity of the particles
- The interface particles/host medium.

Several models have been developed in the literature (Bruggeman 1935; Nan *et al.* 1997; Chen 1998; Wang *et al.* 2007; Behrang *et al.* 2013; Guo and Wang 2015; Zhang and Minnich 2015) but the originality of the present work is that it is based on Extended Irreversible Thermodynamics (EXIT) (Jou *et al.* 2010; Lebon and Machrafi 2015; Lebon *et al.* 2015). At

nanoscales, the transport is not only governed by diffusive collisions between heat carriers but mainly by ballistic collisions. Diffusive collisions refer to collisions experimented by the carriers inside the system whereas ballistic phonons travel more or less freely through the system and undergo collisions with the boundaries. Ballistic collisions are dominant at small length-scales and very low temperatures. As a consequence, the classical Fourier law

$$\mathbf{q} = -\lambda \nabla T \tag{1}$$

relating linearly the heat flux vector $\mathbf{q}$ to the gradient of temperature T, with λ the thermal conductivity, is no longer valid for at least two reasons: first, it does not contain non-local terms and, second it does not account for the finite relaxation time τ of heat carriers. Although this latter property is included in the expression of the Cattaneo equation (Cattaneo 1948)

$$\tau d_t \mathbf{q} + \mathbf{q} = -\lambda \nabla T \tag{2}$$

where d_t stands for time derivative, note that Cattaneo's relation is not designed for non-local phenomena.

There exists several ways to solve the problem, for instance by constructing ad hoc models, but this is not convincing as these models are only applicable to a reduced number of systems and there is generally no physical background. Another solution is to start from the kinetic theory and to solve Boltzmann's equation for phonons. But its resolution is not an easy task and moreover, it is not well adapted to engineering configurations. Another route is to mix kinetic theory and macroscopic approach as suggested by Behrang *et al.* (2013) at Ecole Polytechnique de Montréal. Here a different way is selected consisting in mixing the so-called Effective Medium Approximation (EMA) with EXIT.

The paper is organized as follows. After recalling the main ideas underlying EMA and EXIT in Sections **2** and **3**, we apply our model to the concrete problem of spherical particles dispersed in homogeneous non-metallic materials. The results are extended in Section **4** to cylindrical nanowires. In Section **5** the role of porous nanoparticles is investigated and two applications are proposed. Final remarks and prospectives are found in Sections **6** and **7**.

2. EXIT and EMA formalisms

Let us briefly recall the main ingredients of these two theories. Concerning EXIT, its fundaments and applications have been developed in several books (Müller and Ruggeri 1998; Lebon *et al.* 2008; Jou *et al.* 2010; Ruggeri and Sugiyama 2015; Sellitto *et al.* 2016).

2.1. A brief description of EXIT. The basic idea is to extend the space of state variables by comparison with the classical theory of non-equilibrium thermodynamics based on the local equilibrium hypothesis (Prigogine 1961; De Groot and Mazur 1962). Denoting by x the space of state variables, it is assumed that it is formed by the union of the space $\mathbf{C}$ of classical variables and $\mathbf{F}$, the space of flux variables:

$$x = \mathbf{C} \bigcup \mathbf{F}. \tag{3}$$

The classical variables $\mathbf{C}$ are essentially the mass, the momentum and the energy densities, they are slow and conserved quantities. The flux variables $\mathbf{F}$ are their corresponding fluxes:

fluxes of mass, momentum, energy and eventually higher order fluxes, as the flux of the energy flux, the flux of the flux, ... etc. These variables are fast and non-conserved.

The second important feature is that it is assumed that there exists a non-equilibrium entropy $s(x)$ dependent on the whole set x of variables and whose time variation is given by

$$d_t s = -\nabla \cdot \mathbf{J}^s + \sigma^s \quad (\sigma^s \geq 0). \tag{4}$$

In (4), s is measured per unit volume, σ^s is its rate of production per unit time and unit volume and $\mathbf{J}^s$ is the entropy flux vector. Moreover, σ^s is a non-negative quantity to satisfy the second law of thermodynamics. The time-evolution of the state variables are of the form

$$d_t x = X\left(x, \nabla x, \nabla^2 x, \ldots\right) \tag{5}$$

they are obtained by exploiting the restrictions placed by $\sigma^s \geq 0$ (Jou *et al.* 2010) or by using Liu's more sophisticated technique (1972).

2.2. The EMA approach. The basic idea can be traced back to Maxwell (1881) and Bruggeman (1935), Maxwell's objective was to calculate the electrical conductivity of a system of electrical particles dispersed in an electrolyte. It was more recently generalized to thermal transport among others by Nan *et al.* (1997) and Chen (1998). EMA consists essentially in an homogenization process: the *heterogeneous* two-phase nanocomposite formed of nanoparticles and a host matrix is substituted by a *homogeneous* medium characterized by specific effective properties. In the case of heat transfer, the most relevant quantity is the thermal conductivity to which is devoted the essential of this work. For pedagogical reasons, we will not enter into general considerations, but prefer rather to apply EMA's technique to several examples discussed in the foregoing sections.

3. Rigid spherical nanoparticles dispersed in a homogeneous non-metallic matrix

3.1. General considerations. As a first application, let us consider spherical non-porous nanoparticles of radius r_p dispersed uniformly in a homogeneous non-metallic matrix. With respect to Maxwell's original formulation (1881), a modified EMA description was proposed later on by Nan *et al.* (1997) and revisited by Minnich and Chen (2007). Following these authors, a closed formulation of the effective thermal conductivity λ_{eff} can be written as

$$\lambda_{eff} = \lambda_m \frac{(1+2\alpha)\lambda_p + 2\lambda_m + 2\varphi\left[(1-\alpha)\lambda_p - \lambda_m\right]}{(1+2\alpha)\lambda_p + 2\lambda_m - \varphi\left[(1-\alpha)\lambda_p - \lambda_m\right]}. \tag{6}$$

In (6), λ_m designates the heat conductivity of the matrix, λ_p, the heat conductivity of the particles, φ, the volume fraction of the particles (V_p (particles)/ V(total)) and

$$\alpha = R\lambda_m / r_p \tag{7}$$

is a dimensionless parameter describing the particle-matrix interactions at the interface, with R the thermal boundary resistance (TBR). When a heat flow $\mathbf{q}$ crosses two different materials, there is a barrier across which is observed a temperature drop ΔT with R defined

by $R = \Delta T/\mathbf{q}$. TBR is sensitive to the interfacial density Φ, *i.e.*, the interfacial scattering area of the particles per unit volume. In the case of spherical particles, it is easily checked that

$$\Phi = 3\varphi/r_p \tag{8}$$

meaning that TBR is the largest when the volume fraction is high and the size of particles is small. The coefficient R has been calculated by Chen (1998) from the kinetic theory in terms of the heat capacities c^v and the respective group velocities v_p and v_m of phonons in the particles and the matrix: $R = 4\left(1/c_p^v v_p + 1/c_m^v v_m\right)$. TBR depends of course on the physical nature of the interface, which is described by the so-called specularity parameter s taking values between 0 and 1: $s = 0$ corresponds to a rough surface with incident phonons isotropically diffused through the whole space while the opposite case, $s = 1$, refers to a smooth surface (like a mirror), with phonons reflected in a given direction. To take the specularity into account, the particle radius r_p is redefined as

$$r_p^s = \frac{1+s}{1-s} r_p. \tag{9}$$

In expression (6) of the effective thermal conductivity, there remains two important quantities to be determined, namely the thermal conductivities λ_m and λ_p of the matrix and the particles. Concerning the former, we will use the classical expression drawn from the kinetic theory, namely

$$\lambda_m = (1/3) c_m^v v_m l_m \tag{10}$$

with l_m designating the mean free path of the phonons in the matrix and derived by Minnich and Chen (2007) from Matthiesen rule as

$$1/l_m = 1/l_{m,bulk} + 3\varphi/4r_p \tag{11}$$

the last term being introduced to take into account the collisions of the phonons with the particles in the host phase.

We next determine the thermal conductivity of the nanoparticles, it is at this level that we refer to EXIT. As the details of the derivation have been given explicitly elsewhere (Jou *et al.* 2010; Lebon and Machrafi 2015; Lebon *et al.* 2015) we will here only recall the main steps.

Step 1: we consider an infinite number of state variables $\mathbf{q}$, $\mathbf{Q}^{(2)}$, ... $\mathbf{Q}^{(n)}$ $(n \to \infty)$ with $\mathbf{Q}^{(2)}$, $\mathbf{Q}^{(3)}$, ... designating the flux of the heat flux, the flux of the flux of the heat flux, etc.

Step 2: we formulate the corresponding linear time–evolution equations subject to the restrictions placed by the positiveness of the entropy production.

Step 3: applying Fourier's transform $\hat{\mathbf{q}}(\mathbf{k},t) = \int_{-\infty}^{+\infty} \mathbf{q}(\mathbf{r},t) e^{-i\mathbf{k}\cdot\mathbf{r}} d\mathbf{r}$, $\mathbf{k}$ designating the wave number vector and $\mathbf{r}$ the position vector, we are led after some lengthy but elementary calculations to a Cattaneo-like equation for the Fourier transform $\hat{\mathbf{q}}$,

$$\tau d_t \hat{\mathbf{q}}(\mathbf{k}) + \hat{\mathbf{q}}(\mathbf{k}) = -i\mathbf{k}\lambda_p(\mathbf{k})\hat{T}(\mathbf{k}), \tag{12}$$

wherein the wave-dependent heat conductivity $\lambda_p(\mathbf{k})$ is given by a continuous fraction

$$\lambda_p(\mathbf{k}) = \frac{\lambda_0}{1+\frac{k^2 l_1^2}{1+\frac{k^2 l_2^2}{1+\frac{k^2 l_3^2}{1+\ldots}}}}, \tag{13}$$

with λ_0 the bulk thermal conductivity, that will be given by (10), and the correlation lengths l_n related to the mean free path l_p of the phonons in the particles by $l_n^2 = l_p^2(n+1)^2/(4(n+1)^2-1)$. Note that due to (13), Eq. (12) is not strictly the Cattaneo equation, but actually takes into account the non-local effects.

Step 4: as there is only one single length involved in the problem, namely the radius of the particles, it is natural to identify the wave vector with a scalar k as given by $k = 2\pi/r_p$.

Step 5: for further purpose, let us introduce the so-called Knudsen number Kn defined as

$$Kn = l_p/r_p. \tag{14}$$

In classical situations for which the dimensions are much larger than the mean free path of the heat carriers, Kn is much smaller than one, whereas for small systems, such as nanoparticles, Kn is larger than one.

Step 6: In the asymptotic limit $n \to \infty$, and following a procedure similar to that developed by Hess (1977), the continuous fraction (13) can be written as

$$\lambda_p = (\frac{1}{3}c_p^v v_p l_p)\frac{3}{4\pi^2 Kn^2}\left[\frac{2\pi Kn}{arctan(2\pi Kn)} - 1\right]. \tag{15}$$

The term between parentheses represents the bulk contribution whereas the remaining terms describe the size effects of the nanoparticles through the Knudsen number. Expression (15) is the most important result of the present analysis. We now apply it to some illustrative examples.

3.2. Si nanoparticles dispersed in a Ge matrix. In Fig. 1, we have represented the effective thermal conductivity versus the volume fraction for three values of the specularity parameter ($s = 0$, 0.2, 1) and three different radii ($r_p = 5, 25$ and 100 nm) of the spheres assumed to be uniformly dispersed in the host medium. The results are valid at room temperature.

It may appear as a paradox that the thermal conductivity of the two-phase system Si/Ge is smaller than that of the matrix Ge, at least for s different from $s = 1$, indeed the bulk heat conductivity Ge is 60 W/mK and that of Si is 126 W/mK. This peculiarity is interpreted by the fact that by increasing the volume fraction, one increases the interfacial density (see Eq. (8)) and similarly the thermal boundary resistance, whence a reduction of the thermal conductivity. The figures $1_{(b)}$ and $1_{(c)}$ indicate that the thermal conductivity is increased with larger sizes because the effective interfacial boundary is actually decreased (see Eq. (8)). In the limiting case $s = 1$, Eq. (9) predicts that r_p^s tends to infinity, which amounts to a vanishing scattering interface. The results are in very good agreement with these obtained

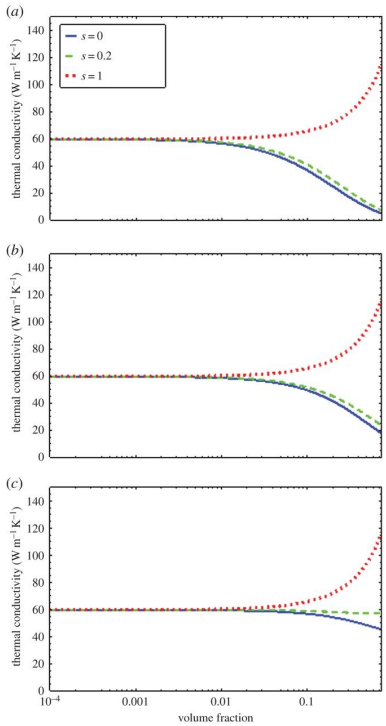

FIGURE 1. Effective thermal conductivity of Si/Ge as a function of the specularity parameter and three different nanoparticle's radii: (a) 5 nm, (b) 25 nm and (c) 100 nm. [Republished with permission of The Royal Society, from "An extended irreversible thermodynamic modelling of size-dependent thermal conductivity of spherical nanoparticles dispersed in semi-conductors", Lebon, G., Machrafi, H., and Grmela, M., Proceedings of The Royal Society A **471**, 20150144, 2015; permission conveyed through Copyright Clearance Center, Inc.].

by other models (Minnich and Chen 2007; Behrang *et al.* 2013)), experimental data and Monte Carlo simulations (Machrafi and Lebon 2014; Lebon *et al.* 2015).

3.3. SiO_2 **(silicate) nanoparticles embedded in epoxy resin.** The results of Fig. 2 indicate that, contrary to the previous example, the effective thermal conductivity is now growing with increasing volume fraction. This is so because the heat conductivity of the nanoparticles is much larger (by a factor 10 at least) than that of the matrix and will therefore dictate its behavior; in particular, the higher is the silicate particles density, the larger is the thermal conductivity.

The right frame of the Fig. 2 is a zooming of the results in the region $0 < \varphi < 0.1$, and the circles denote experimental results. As indicated above, thermal conductivity is now growing with the particles density. It is also worth to stress that an excellent agreement with experiments is observed.

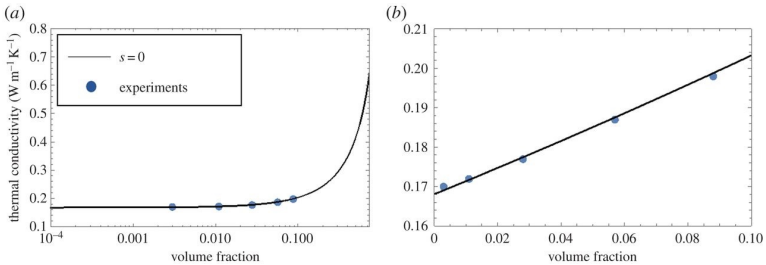

FIGURE 2. Effective thermal conductivity of SiO_2 embedded in epoxy resin for $s = 0$ (rough diffusive surface) and $r_p = 10$ nm. [Republished with permission of The Royal Society, from "An extended irreversible thermodynamic modelling of size-dependent thermal conductivity of spherical nanoparticles dispersed in semi-conductors", Lebon, G., Machrafi, H., and Grmela, M., Proceedings of The Royal Society A **471**, 20150144, 2015; permission conveyed through Copyright Clearance Center, Inc.].

3.4. AlN (aluminium nitride) embedded in epoxy resin. The results plotted in Fig. 3 indicate that the model underestimates the experimental data.

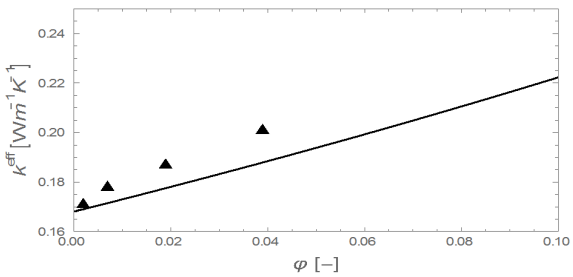

FIGURE 3. Effective thermal conductivity versus the volume fraction for $s = 0$ and $r_p = 11$ nm, triangles represent experimental data [Reprinted from "Effect of volume-fraction dependent agglomeration of nanoparticles on the thermal conductivity of nanocomposites: Applications to epoxy resins, filled by SiO2, AlN and MgO nanoparticles", Machrafi, H., Lebon, G., and Iorio, C., Composites Science and Technology **130**, 78–87, 2016; with permission from Elsevier.]

Disagreement with experiments may be due to the fact that the dispersion of particles is no longer uniform. Indeed recent investigations at the experimental and theoretical levels (Machrafi *et al.* 2016a) have shown that agglomeration of particles is important in this nanocomposite and that the formation of clusters plays a decisive role in heat transport.

3.5. Temperature dependence in Si/Ge. Up to now, the temperature was fixed equal to the room temperature 300 K. The results of Section **3.1** have been generalized by Lebon *et al.* (2015) to study the role of temperature. The results are reproduced in Fig. 4.

We have represented in Fig. 4 the behavior of λ_{eff} versus the temperature for $s = 0$, three values of the volume fraction and three different nanoparticles sizes: 5, 25, and 100

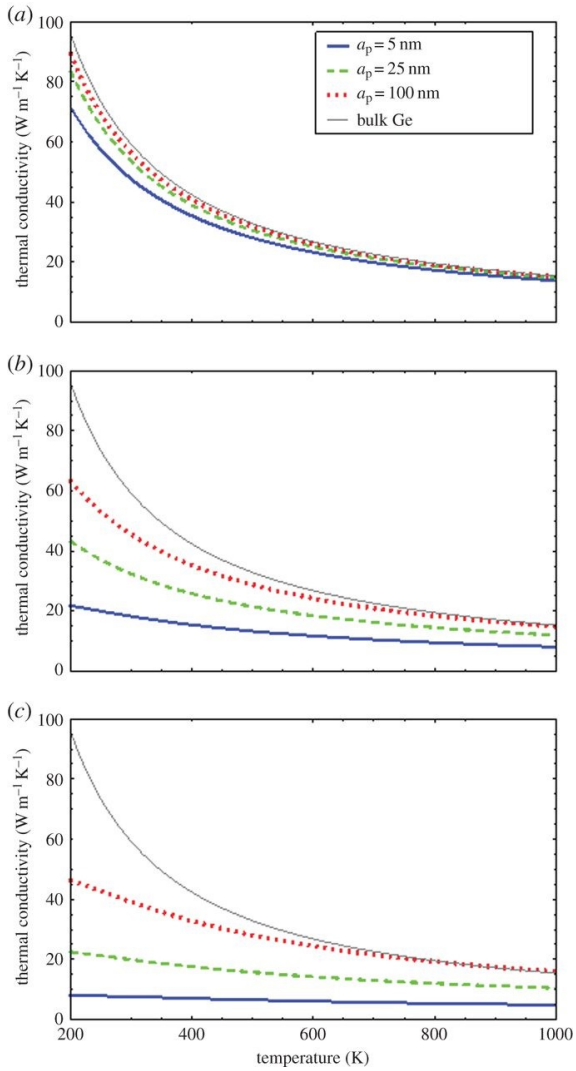

FIGURE 4. Effective thermal conductivity of Si/Ge as a function of temperature T for various Si particles' radii (denoted here by a) and three different values of the volume fraction, (a) $\varphi = 0.01$, (b) $\varphi = 0.2$ and (c) $\varphi = 0.5$, s is fixed at $s = 0$. [Republished with permission of The Royal Society, from "An extended irreversible thermodynamic modelling of size-dependent thermal conductivity of spherical nanoparticles dispersed in semi-conductors", Lebon, G., Machrafi, H., and Grmela, M., Proceedings of The Royal Society A **471**, 20150144, 2015; permission conveyed through Copyright Clearance Center, Inc.].

nm, respectively, three different volume fractions for the sake of comparison, we have also drawn the curve corresponding to bulk Ge. Increasing the temperature induces a reduction of the mean free path of the phonons and therefore a reduction of the heat conductivity as shown by formula (10). One observes indeed a decrease of λ_{eff} with increasing temperature whatever the volume fraction and the radius of the particles. Moreover the influence of the particle's size becomes less important as the temperature is higher. At high temperature the phonons-boundary collisions are less frequent than the bulk phonon-phonon scattering and therefore the sensitivity of heat conductivity to the size of the particles is weaker.

4. Tubular nanowires composites

The considerations of the previous section are now extended to cylindrical nanowires of radius r_p and length L, uniformly dispersed in homogeneous supports. EMA approach distinguishes heat fluxes normal $\perp$ and parallel $\|$ to the cylinder axis of symmetry, following Nan *et al.* (1997), the corresponding effective thermal conductivities are respectively given by

$$\begin{aligned} \lambda_{\perp}^{eff} &= \lambda_m \frac{(1+\alpha)\lambda_p+\lambda_m+\varphi\left[(1-\alpha)\lambda_p-\lambda_m\right]}{(1+\alpha)\lambda_p+\lambda_m-\varphi\left[(1-\alpha)\lambda_p-\lambda_m\right]} \\ \lambda_{\|}^{eff} &= (1-\varphi)\lambda_m+\varphi\lambda_p \end{aligned} . \tag{16}$$

We have used the same notation as for spherical particles. As illustration, we have calculated the transversal effective thermal conductivity of the couple Si/Ge for three different values of r_p and have compared the results with these derived from Fourier's law and the case $\alpha = 0$ (no boundary resistance). The results (Lebon and Machrafi 2015) are gathered in Fig. 5.

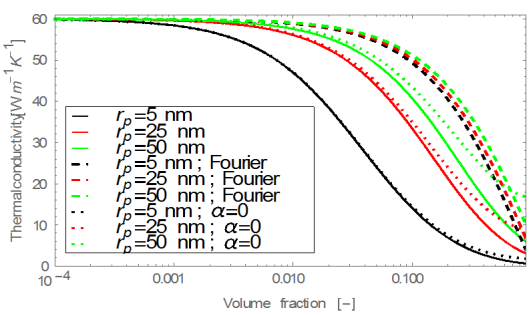

FIGURE 5. Effective transversal thermal conductivity as a function of the volume fraction for 3 values of r_p (5, 25, 50 nm) and diffusive interface ($s = 0$): our model is indicated by solid lines, the Fourier model by dashed ones and the one with no boundary resistance ($\alpha = 0$) by dotted lines. [Reprinted from "Thermal conductivity of tubular nanowire composites based on a thermodynamical model", Lebon, G. and Machrafi, H., Physica E **71**, 117–122, 2015; with permission from Elsevier.]

The following remarks are in form:

(1) the thermal conductivity decreases with volume fraction,
(2) the thermal conductivity decreases with decreasing particle's size,
(3) differences with Fourier's law (upper curves) are important as they may be of the order of 80%,
(4) the thermal conductivity is, without any surprise, the largest for $\alpha = 0$,
(5) it has been numerically checked that the effects of the longitudinal length L are small.

Similar results are obtained for the longitudinal heat conductivity, as seen in Fig. 6.

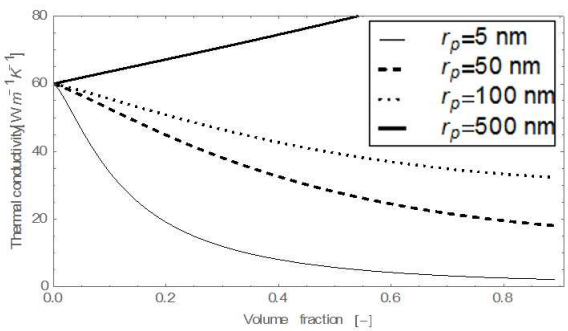

FIGURE 6. Effective parallel thermal conductivity λ_{eff} versus volume fraction φ for four different radii. [Reprinted from "Thermal conductivity of tubular nanowire composites based on a thermodynamical model", Lebon, G. and Machrafi, H., Physica E **71**, 117–122, 2015; with permission from Elsevier.]

It is still noticed that generally λ_{eff} decreases with φ and, at fixed φ, increases with increasing size. In contrast, the conductivity increases at large r-values, say 500 nm (see the upper the bold line). At such values, the Knudsen number $Kn << 1$ from which follows that we are in the Fourier regime with the heat conductivity growing with the particles density (the non-local effects become negligible).

5. The role of porosity

In this section, the role of porosity of nanoparticles and nano-porous systems will receive a special treatment and two specific applications are briefly discussed.

5.1. Heat conductivity of nanoporous Si. We consider spherical nano-pores uniformly dispersed in a Si matrix, the nano-porous inclusions are assumed to be filled by air, for illustration. The effective thermal conductivity of the system is given by expression (6) wherein the volume fraction φ is replaced by the porosity ε, defined as the ratio of the volume occupied by the pores and the total volume:

$$\lambda_{eff} = \lambda_m \frac{(1+2\alpha)\lambda_p + 2\lambda_m + 2\varepsilon\left[(1-\alpha)\lambda_p - \lambda_m\right]}{(1+2\alpha)\lambda_p + 2\lambda_m - \varepsilon\left[(1-\alpha)\lambda_p - \lambda_m\right]} \tag{17}$$

λ_m is the thermal conductivity of bulk Si and λ_p that of the nano-pores expressed by relation (15) with λ^0 (substituted to the kinetic result $\frac{1}{3}c^v vl$) standing for the heat conductivity of air, namely $\lambda^0 = 0.0026$ W/mK.

The validity of our model is evaluated by comparing our results with the hydrodynamic model (Alvarez *et al.* 2010), consisting in a kinetic version of Stokes' resistance force. Accordingly, the thermal conductivity is given by

$$\lambda_{eff}^{hydro} = \lambda_m \left(\frac{1}{(1-\varepsilon)^3} + \frac{9\varepsilon}{2} \frac{Kn^2}{1+Kn-(0.864+0.29e^{-1.25Kn})} \left(1+\frac{3\sqrt{5}}{\sqrt{2}}\right)\right)^{-1} \tag{18}$$

Letting Kn tend to zero leads to the well-known percolation model

$$\lambda_{eff} = \lambda_m^0 (1-\varepsilon)^3 \tag{19}$$

In Fig. 7, the results of our model are compared with the hydrodynamic one and experimental data in the case of four pore radii: 2, 5, 10 and 100 nm.

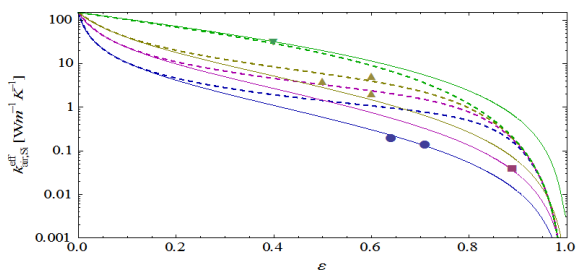

FIGURE 7. Effective thermal conductivity versus porosity for two models, several pore sizes (2 nm (blue line), 5 nm (qarnet line), 10 nm (brown line) and 100 nm (green line)) and experimental data (symbols). Our model is indicated by solid lines and the hydrodynamic model by dashed lines. [Reprinted from "Size and porosity effects on thermal conductivity of nanoporous material with an extension to nanoporous particles embedded in a host matrix", Machrafi, H. and Lebon, G., Physics Letters A **379**, 968–973, 2015; with permission from Elsevier.]

The general trend is a decrease of heat conductivity with porosity whatever the model, and that at fixed porosity, heat conductivity is considerably reduced by passing from larger pores to smaller ones in the nanosize range. We observe, however, rather important differences between both models in the region of mid-porosities ($0.2 < \varepsilon < 0.9$). A better agreement between our model and experimental data is observed, especially at higher porosities. To close this section, let us discuss two interesting applications.

5.2. Porous Si nanoparticles embedded in Ge. In Section **3.2**, we have calculated the effective thermal conductivity of solid (without porosity) Si nanoparticles dispersed in a Ge matrix. We now repeat the exercise by considering instead, porous Si nanoparticles filled by air uniformly distributed in Ge. The results are represented in Fig. 8, as a function of the

volume fraction φ of nanoparticles and different values of the porosity. For details of the calculations, we refer to Machrafi and Lebon (2015).

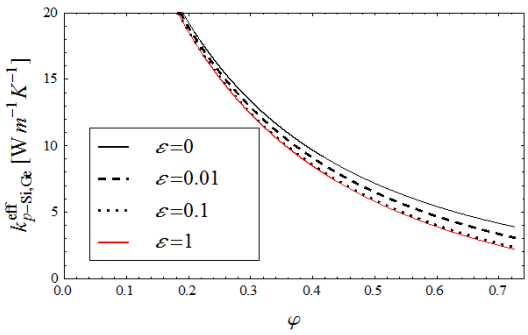

FIGURE 8. Effective thermal conductivity of Si/ Ge as a function of volume fraction of Si particles for different values of the porosity: $\varepsilon = 0$ (bulk Si), 0.01, 0.1 and 1 (air bubbles in Ge), with r_p (Si particle radius) = 25 nm and a_p (pore size) = 1 nm.[Reprinted from "Size and porosity effects on thermal conductivity of nanoporous material with an extension to nanoporous particles embedded in a host matrix", Machrafi, H. and Lebon, G., Physics Letters A **379**, 968–973, 2015; with permission from Elsevier.]

It is shown that k^{eff}, decreases with increasing volume fraction and that it is rather insensitive to the porosity: indeed a porosity of 0.1 yields results practically equivalent to bulk particles. This is however no longer true by increasing the radius of the Si nanoparticles, for instance at $r_p = 100$ nm, the reduction of thermal conductivity becomes stronger as porosity is increased. This is visible in Fig. 9.

5.3. Thermal rectifiers. Thermal rectifiers are devices allowing the heat to flow in one direction but blocking it in the opposite direction: they are the analogs of diodes in electricity. The important factor is the dimensionless thermal rectifying coefficient **R*** defined by

$$\mathbf{R}^* = \frac{\|\mathbf{q}_d\|}{\|\mathbf{q}_r\|} \tag{20}$$

with $\mathbf{q}_d$ denoting the heat flow in the direct direction and $\mathbf{q}_r$ the flow in the reverse direction. To have rectification, the coefficient **R*** must be larger than 1. Experimental devices have exhibited values up to 2.2 but recently, a solid state structure with shape memory alloys recorded an **R***-value of the order of 90. A problem of actual interest is to find the best configuration among several bulk–nanoporous devices giving the highest **R***-value. The subject has been recently treated by Machrafi *et al.* (2016b) and is commented in Jou *et al.* (2018).

6. Flashback

Our objective was to model the effective thermal conductivity of non-metallic nano-composites, constituted by nanoparticles uniformly dispersed in homogeneous polymers or

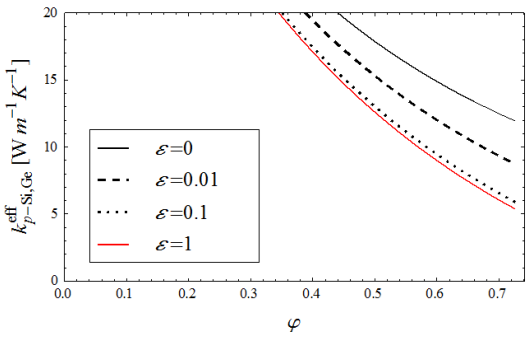

FIGURE 9. Effective thermal conductivity of Si/Ge as a function of volume fraction of Si particles for different values of the porosity: $\varepsilon = 0$ (bulk Si), 0.01, 0.1 and 1 (air bubbles in Ge), with r_p (Si particle radius) = 100 nm and a_p (pore size) = 1 nm.[Reprinted from "Size and porosity effects on thermal conductivity of nanoporous material with an extension to nanoporous particles embedded in a host matrix", Machrafi, H. and Lebon, G., Physics Letters A **379**, 968–973, 2015; with permission from Elsevier.]

semiconductors. This has been achieved by mixing the Effective Medium Approximation (EMA) and Extended Irreversible Thermodynamics (EXIT). The originality of the model is the derivation of the thermal conductivity of the particles on the bases of EXIT. The most important results of this work are embedded in Eqs. (6) and (15). A particular attention has been put on spherical and porous nanoparticles and tubular wires. Illustrations have concerned not only Si, SiO_2 and AlN nanoparticles dispersed in Ge and epoxy resin, but also nanoporous Si embedded in Ge. We have studied the sensitivity of the effective thermal conductivity to the nature, volume fraction, size and porosity of nanoparticles, the effect of temperature has also been analyzed. The main results are summarized below:

- A decrease (or increase) of effective heat conductivity with increasing volume fraction, depends on the nature of the nanocomposite. Increase or decrease is essentially conditioned by the value of the coefficient α (see Eq. (7)), expressing the interactions at the interface. For $\alpha > 1$ (high thermal boundary resistance (TBR) and small particles' size) λ_{eff} is decreasing while it is increasing for $\alpha < 1$ (weak TBR and large particles' size). The value of the α-parameter is of importance within the perspective of practical applications: constituents with small α-values should be selected when significant enhancement of the thermal conductivity is aimed at, like in electronic devices wherein evacuation of heat is required, large values of α should be preferred when a reduction of heat transport is the objective, for instance with the perspective of increasing thermal isolation, or in thermoelectric devices.
- A decrease of effective heat conductivity with decreasing particle size.
- A decrease of effective heat conductivity with increasing temperature.
- A decrease of effective heat conductivity with increasing porosity.

A good agreement has been observed with experimental data, Monte-Carlo simulations and other models.

7. Back to the future (open problems)

A series of problems to be investigated in the future are, among others:

- To mix nanoparticles of different nature, shape and size.
- To include non-linear contributions involving terms in $\mathbf{q}^2$, $\mathbf{q} \cdot \nabla \mathbf{q}$, .. in the time evolution equations of the fluxes.
- To apply the analysis to other configurations as thin films and superlattices.
- To extend the above considerations to nanofluids, wherein specific effects as Brownian motion, presence of boundary layers around the particles, and formation of clusters are to be taken into account (Machrafi and Lebon 2016).
- To exploit the property of decreasing heat conductivity to enhance the figure of merit Z of thermoelectric devices which is inversely proportional to the thermal conductivity.
- To study thermal conductivity of concentrated media, including percolation phenomena.
- To generalize the above technique to other transport coefficients like electrical conductivity, thermoelectric coefficients and viscosity of nanofluids.
- To investigate complex configurations including both nanoparticles and nanopores.

Acknowledgements

The present work was presented at the Thermocon 16th International Conference held in Messina from 19 to 22 April, 2016. G.L wishes to thank the organizers profs. L. Restuccia and V. Ciancio for their kind invitation to participate to this meeting. The present work is performed in the frame of the Wallonie-Bruxelles-Québec project, 9th CMP RI 15.

References

Alvarez, F., Jou, D., and Sellitto, A. (2010). "Pore-size dependence of the thermal conductivity of porous silicon: A phonon hydrodynamic approach". *Applied Physics Letters* **97**, 033103. DOI: 10.1063/1.3462936.

Behrang, A., Grmela, M., Dubois, C., Turenne, S., and Lafleur, P. (2013). "Influence of particle–matrix interface, temperature and agglomeration of heat conduction in dispersions". *Journal of Applied Physics* **114**, 014305. DOI: 10.1063/1.4812734.

Bruggeman, D. (1935). "Berechnung verschiedener physikalischer Konstanten von heterogenen Substanzen". *Annalen der Physik* **416**, 636–664. DOI: 10.1002/andp.19354160705.

Cattaneo, C. (1948). "Sulla conduzione del calore". *Atti Seminario Matematico Fisico Università Modena* **3**, 83–101.

Chen, G. (1998). "Thermal conductivity and ballistic-phonon transport in the cross-plane direction of superlattices". *Physical Review B* **57**, 14958–14973. DOI: 10.1103/PhysRevB.57.14958.

De Groot, S. and Mazur, P. (1962). *Non–Equilibium Thermodynamics*. North-Holland Publishing.

Guo, Y. and Wang, M. (2015). "Phonon hydrodynamics and its applications in nanoscale heat transport". *Physics Reports* **595**, 1–44. DOI: 10.1016/j.physrep.2015.07.003.

Jou, D., Casas-Vazquez, J., and Lebon, G. (2010). *Extended Irreversible Thermodynamics*. Springer. DOI: 10.1007/978-90-481-3074-0.

Jou, D., Sciacca, M., Sellitto, A., and Galantucci, L. (2018). "Refrigeration bound of heat-producing cylinders by superfluid helium". *Atti della Accademia Peloritana dei Pericolanti. Classe di Scienze Fisiche, Matematiche e Naturali*. DOI: 10.1478/AAPP.xxxxx.

Lebon, G., Jou, D., and Casas-Vazquez, J. (2008). *Understanding Non-equilibrium Thermodynamics*. Springer. DOI: 10.1007/978-3-540-74252-4.

Lebon, G. and Machrafi, H. (2015). "Thermal conductivity of tubular nanowire composites based on a thermodynamical model". *Physica E* **71**, 117–122. DOI: 10.1016/j.physe.2015.04.008.

Lebon, G., Machrafi, H., and Grmela, M. (2015). "An extended irreversible thermodynamic modelling of size-dependent thermal conductivity of spherical nanoparticles dispersed in semi-conductors". *Proceedings of the Royal Society A* **471**, 20150144. DOI: 10.1098/rspa.2015.0144.

Machrafi, H. and Lebon, G. (2014). "Effective thermal conductivity of spherical particulate nanocomposites: Comparison with theoretical models, Monte Carlo simulations and experiments". *International Journal of Nanoscience* **13**, 1450022. DOI: 10.1142/S0219581X14500227.

Machrafi, H. and Lebon, G. (2015). "Size and porosity effects on thermal conductivity of nanoporous material with an extension to nanoporous particles embedded in a host matrix". *Physics Letters A* **379**, 968–973. DOI: 10.1016/j.physleta.2015.01.027.

Machrafi, H. and Lebon, G. (2016). "The role of several heat transfer mechanisms on the enhancement of thermal conductivity in nanofluids". *Continuum Mechanics and Thermodynamics* **28**, 1461–1475. DOI: 10.1007/s00161-015-0488-4.

Machrafi, H., Lebon, G., and Iorio, C. (2016a). "Effect of volume-fraction dependent agglomeration of nanoparticles on the thermal conductivity of nanocomposites: Applications to epoxy resins, filled by SiO2, AlN and MgO nanoparticles". *Composites Science and Technology* **130**, 78–87. DOI: 10.1016/j.compscitech.2016.05.003.

Machrafi, H., Lebon, G., and Jou, D. (2016b). "Thermal rectifier efficiency of various bulk-nanoporous silicon devices". *International Journal of Heat and Mass Transfer* **97**, 603–610. DOI: 10.1016/j.ijheatmasstransfer.2016.02.048.

Maxwell, J. (1881). *Treatise on Electricity and Magnetism*. Clarendon. DOI: 10.3931/e-rara-8841.

Minnich, A. and Chen, G. (2007). "Modified effective medium formulation for the thermal conductivity of nanocomposites". *Applied Physics Letters* **91**, 073105. DOI: 10.1063/1.2771040.

Müller, I. and Ruggeri, T. (1998). *Rational Extended Thermodynamic*. Springer. DOI: 10.1007/978-1-4612-2210-1.

Nan, C., Birringer, R., Clarke, D., and Gleiter, H. (1997). "Effective thermal conductivity of particulate composites with interfacial thermal resistance". *Journal of Applied Physics* **81**, 6692–6699. DOI: 10.1063/1.365209.

Prigogine, I. (1961). *Introduction to Thermodynamics of Irreversible Processes*. Interscience.

Ruggeri, I. and Sugiyama, M. (2015). *Rational Extended Thermodynamics beyond the Monatomic Gas*. Springer. DOI: 10.1007/978-3-319-13341-6.

Sellitto, A., Cimmelli, V., and Jou, D. (2016). *Mesoscopic Theories of Heat Transport in Nanosystems*. Springer. DOI: 10.1007/978-3-319-27206-1.

Wang, M., Wang, J., Pan, N., and Chen, S. (2007). "Mesoscopic predictions of the effective thermal conductivity for microscale random porous media". *Physical Review E* **75**, 036702. DOI: 10.1103/PhysRevE.75.036702.

Zhang, H. and Minnich, A. (2015). "The best nanoparticle size distribution for minimum thermal conductivity". *Scientific Reports* **5**, 8995. DOI: 10.1038/srep08995.

[a] Université de Liège
Institut de Physique
4000 Liège, Belgium

* To whom correspondence should be addressed | email: g.lebon@uliege.be

Paper contributed to the conference entitled "Thermal theories of continua: survey and developments (Thermocon 2016)", which was held in Messina, Italy (19–22 April 2016) under the patronage of the *Accademia Peloritana dei Pericolanti*

Manuscript received 25 October 2017; published online 20 May 2019

© 2019 by the author(s); licensee *Accademia Peloritana dei Pericolanti* (Messina, Italy). This article is an open access article distributed under the terms and conditions of the Creative Commons Attribution 4.0 International License (https://creativecommons.org/licenses/by/4.0/).